In This Lecture:

- Excitons in QWs
- Quantum Confined Stark Effect
- Exciton Quenching
- Excitons in TMDs

Excitons in two-dimensions

There is a good reason for going to lower dimensions for Xs.

This is simply illustrated by comparing solution of H atom in 2D with 3D:

Remember:
H $\rightarrow$ X
$Ry \rightarrow R_{ex}$

$$R_{ex,2D} = 4R_{ex}$$

$$a_{ex,2D} = \frac{a_{ex}}{2}$$

enhanced X binding in 2D

A QW is a quasi-2D structure so: $R_{ex,2D} > R_{ex,QW} > R_{ex}$

Nevertheless, due to enhanced binding a QW X can survive well above room temperatures, depending on the material parameters

Ref: Singh

For a QW grown along *z*-axis the envelope function equation is written as:

$$H = \underbrace{\frac{-\hbar^2}{2m_r^*}\left(\frac{1}{\rho}\frac{\partial}{\partial\rho}\rho\frac{\partial}{\partial\rho}+\frac{1}{\rho^2}\frac{\partial^2}{\partial\phi^2}\right)}_{\text{in-plane: relative coord. use reduced eff. mass}} \underbrace{-\frac{\hbar^2}{2m_e}\frac{\partial^2}{\partial z_e^2}-\frac{\hbar^2}{2m_h}\frac{\partial^2}{\partial z_h^2}}_{\text{confinement direction: treat e \& h separately}} \underbrace{-\frac{e^2}{4\pi\epsilon|\mathbf{r}_e-\mathbf{r}_h|}}_{\text{use still 3D Coulomb}} \underbrace{+V_{ew}(z_e)+V_{hw}(z_h)}_{\text{e \& h QW confinement}}$$

ε: use static dielectric constant when no free carriers are present.
If there are free carriers, they will further screen the e-h Coulombic attraction term until the Mott density, above which QW X becomes unbound (more later)

No simple analytical solution even under EFA+parabolic dispersion (as we do here). One convenient approach for obtaining the envelope fn is to assume a functional form (like Gaussian) containing one variational parameter,and determining it by minimizing the energy:

$$E = \frac{\int \psi_{ex}^* \, H \, \psi_{ex} \, dz_e \, dz_h \, \rho \, d\rho \, d\phi}{\int \psi_{ex}^* \, \psi_{ex} \, dz_e \, dz_h \, \rho \, d\rho \, d\phi}$$

Minimize *E* wrt variational parameter

In practice, X binding energy enhancement in QW (compared to bulk) goes up to ~2.5 rather than 4 as in the ideal 2D case.

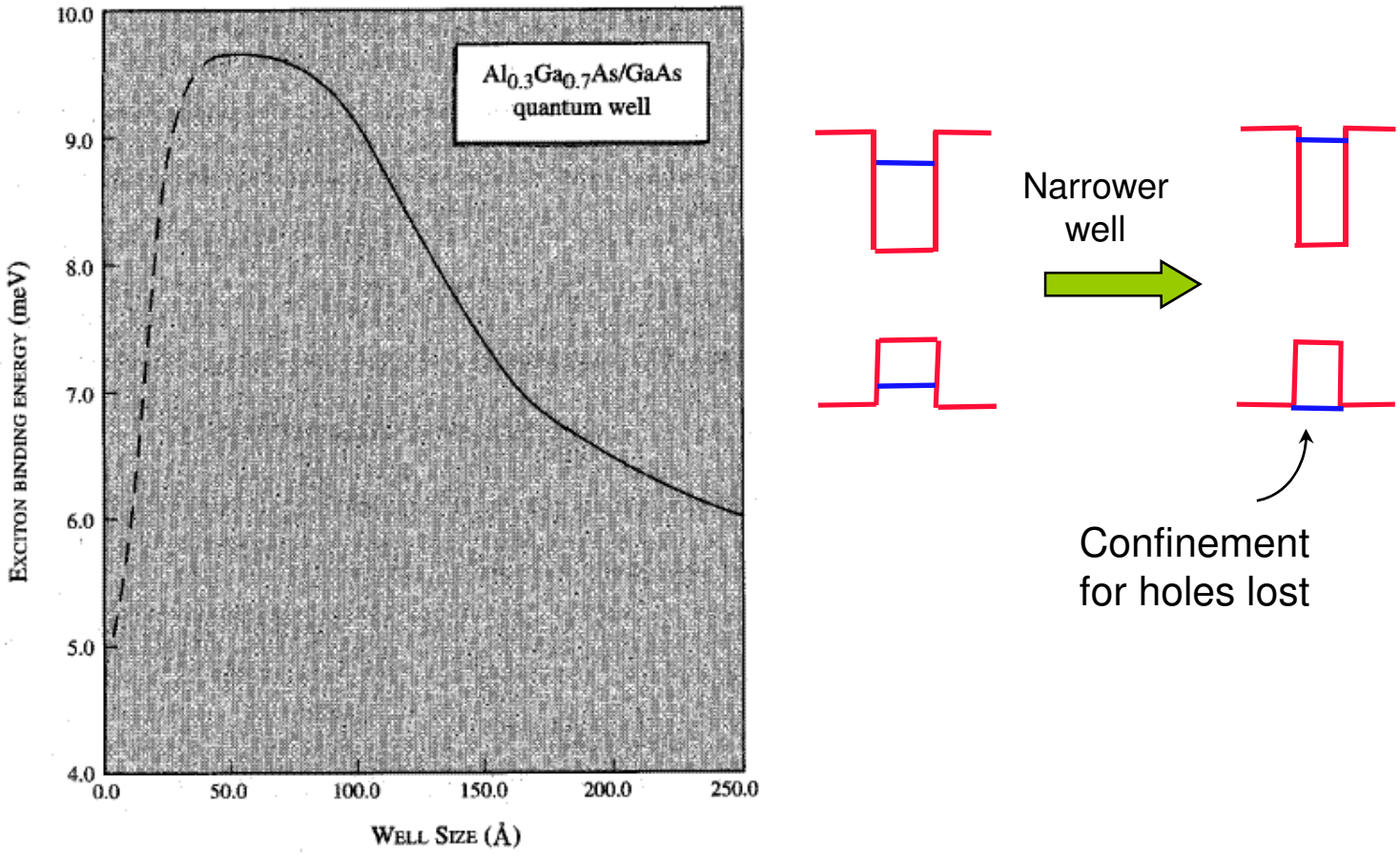

Figure 10.8: Variation of the heavy-hole exciton binding energy as a function of well size in GaAs/$Al_{0.3}Ga_{0.7}As$ wells. The binding energy of the infinite barrier well should approach four times the 3D exciton binding energy as the well size goes to zero.

Ref: Singh

Excitonic Absorption in QWs

Generalize the absorption coef. result of bulk to a QW of size *W:*

$$\alpha^{\text{ex}}(\hbar\omega) = \frac{\pi e^2 \hbar}{n_r m_0^2 c W \hbar\omega} \left| \sum_{\mathbf{k},n,m} \underbrace{G_{nm}(\boldsymbol{k})}_{\text{Fourier xform of the in-plane X envelope fn}} \boldsymbol{a}\cdot\boldsymbol{p}_{nm}(\boldsymbol{k}) \right|^2 \delta(\hbar\omega - E_{nm}^{\text{ex}})$$

Momentum matrix element:

$$\boldsymbol{p}_{nm}(\boldsymbol{k}) = \sum_{\nu,\mu} \int d^2r\, U_0^{\nu}(\boldsymbol{r})\, \boldsymbol{p}\, U_0^{\mu}(\boldsymbol{r}) \int dz\, f_n^{\mu}(z)\, g_m^{\nu}(k,z)$$

The absorption coef. can also be expressed in terms of the oscillator strength as:

$$\alpha^{\text{ex}}(\hbar\omega) = \sum_{nm} \frac{\pi e^2 \hbar}{n_r \epsilon_0 m_0 c W} f_{nm}\, \delta(E_{nm}^{\text{ex}} - \hbar\omega)$$

$$f_{nm} = \frac{2}{m_0 E_{nm}^{\text{ex}} (2\pi)^2} \left| \int d^2k\, G_{nm}(\boldsymbol{k})\, \boldsymbol{a}\cdot\boldsymbol{p}_{nm}(\boldsymbol{k}) \right|^2$$

It does not involve the δ-function term

Ref: Singh

If the 2D X fn can be represented by an X radius a_{ex}, then as in 3D case (also broaden the δ-function with the Gaussian)

$$\alpha^{ex}(\hbar\omega) = \frac{\pi e^2 \hbar}{2 n_r \epsilon_0 c m_0 \hbar\omega} \left(\frac{2|p_{cv}|^2}{m_0}\right) a_p \left(\frac{1}{\sqrt{1.44\pi}} \frac{1}{\sigma} \frac{1}{W \pi a_{ex}^2} \exp\left(\frac{-(\hbar\omega - E_{ex})^2}{1.44\sigma^2}\right)\right)$$

polarization factor

a_{ex} decreases up to a factor of 2 making X absorption peak stronger

Ref: Singh

Modulation of Excitonic Transitions: Quantum Confined Stark Effect (QCSE)

Atomic Stark Effect:

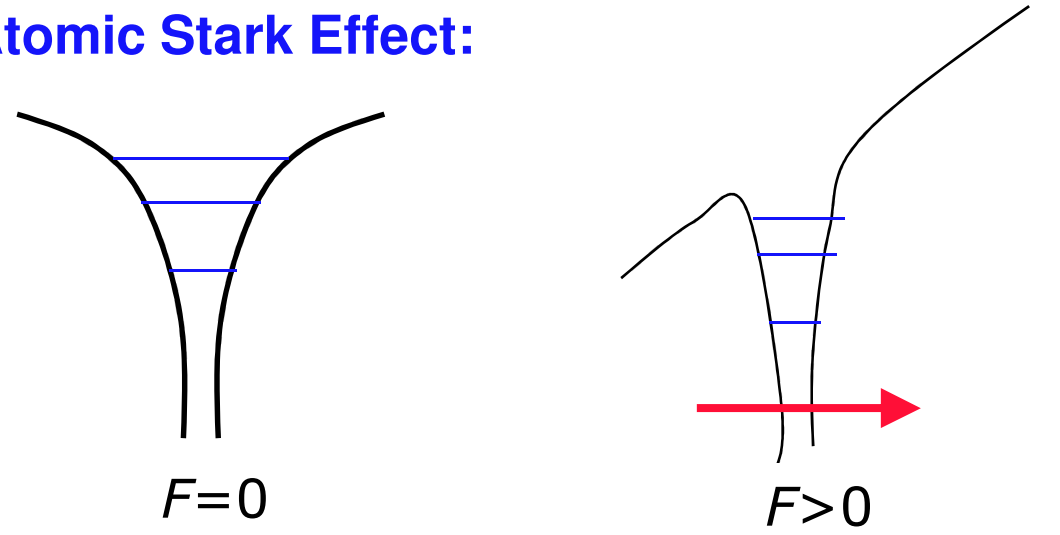

See for eg. Gasiorowicz

QCSE:

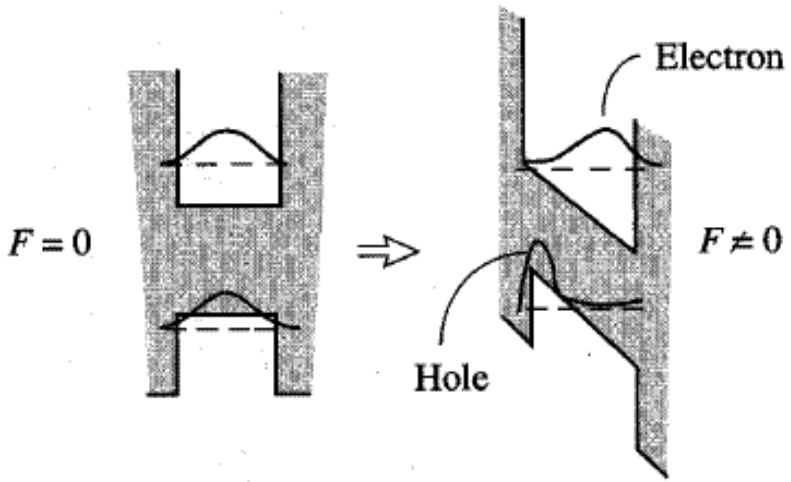

Effects of the External Electric Field:

1) The intersubband separations change; the field pushes the e and h to opposite sides making the ground state intersubband separation smaller. This is the dominant term in changing the X resonance.

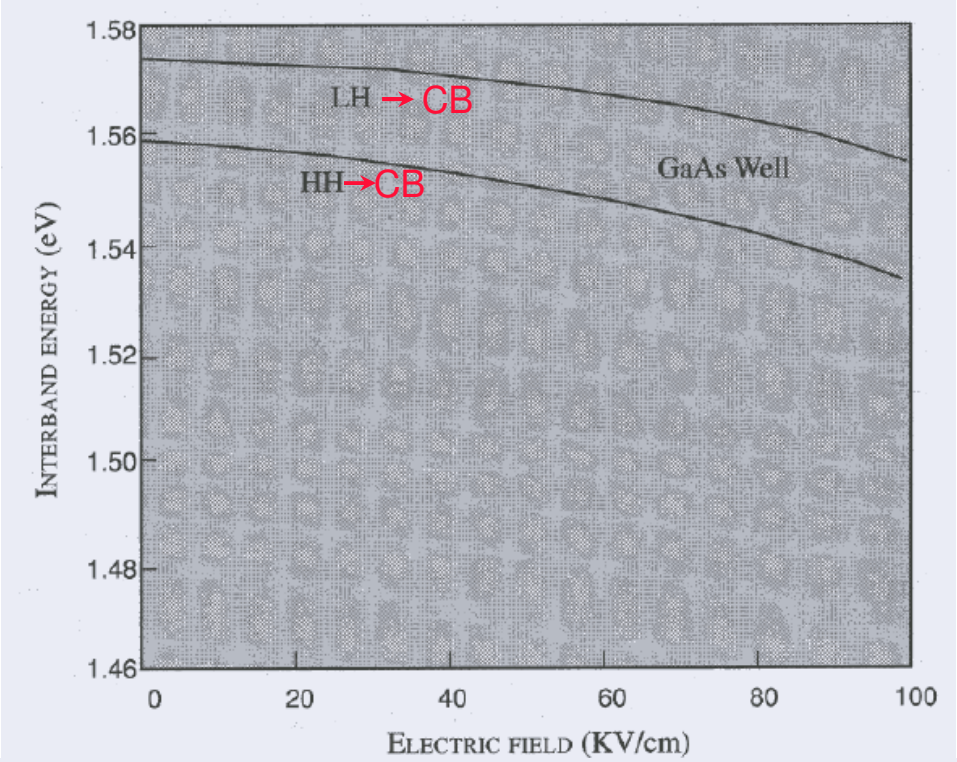

Figure 10.13: Calculated variation of the ground state HH and LH (to conduction band ground state) intersubband transition energies as a function of electric field. The well is a 100 Å $GaAs/Al_{0.3}Ga_{0.7}As$.

Ref: Singh

2) Due to the separation of the e and h wf, the binding energy of the X decreases

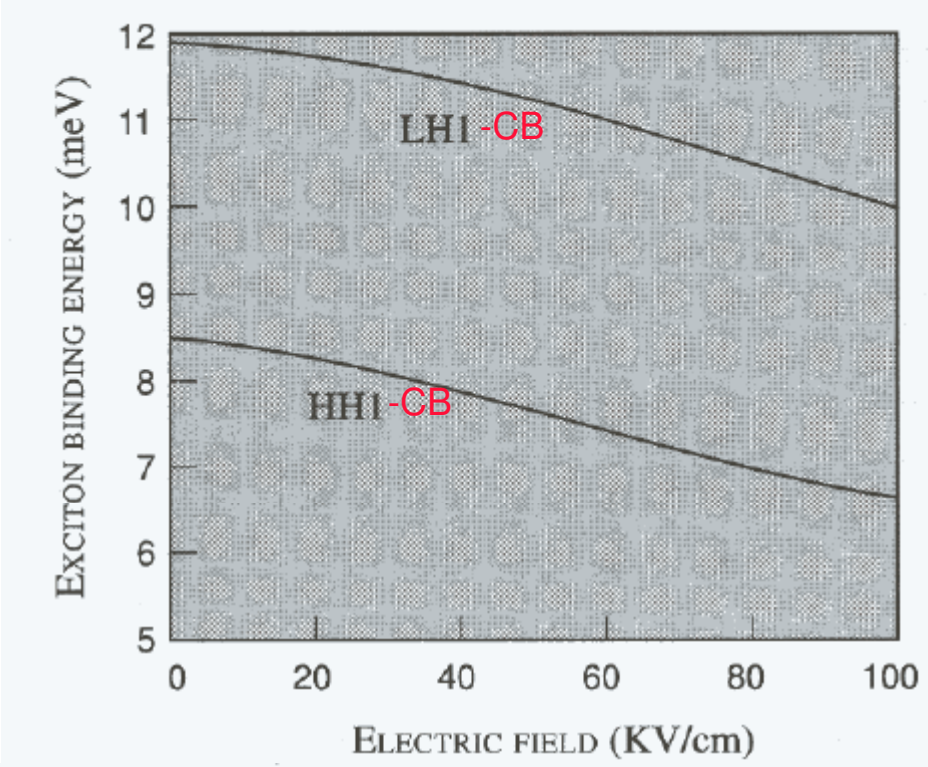

Figure 10.14: Calculated variation in the exciton binding energy in a 100 Å $GaAs/Al_{0.3}Ga_{0.7}As$ quantum well as a function of electric field. The ground state HH and LH exciton results are shown.

As can be seen from the two figures above, the change in X binding energy is only ~2-3 meV while intersubband energies are altered by up to 20 meV. The QCSE is, therefore primarily determined by the intersubband shift.

Ref: Singh

Intersubband shift via Perturbation Theory

Recall that we have considered the very same problem in the discussion of the time independent perturbation theory

$$H = H_0 + eFz$$ → perturbation

$$|eFW| \ll \frac{\hbar^2\pi^2}{2m^*W^2}$$

In the 1st order: $\Delta E^{(1)} = \langle\psi_1|eFz|\psi_1\rangle$ vanishes due to parity

Go to 2nd order: $$\Delta E_1^{(2)} = \frac{1}{24\pi^2}\left(\frac{15}{\pi^2} - 1\right)\frac{m^* e^2 F^2 W^4}{\hbar^2}$$

NB: The shift increases with m^* and has a very strong well size dependence. Recall that X absorption decreases for wider wells; therefore there is a trade off. Optimum QW sizes are of the order of ~ 100 Å (depending on the se/c)

Ref: Singh

Polarization Dependence (QCSE)

Notation

TE (to growth axis): Electric field in QW plane

TM (to growth axis): Electric field along growth axis

Same polarization selection rules apply as the QW interband transitions. So, recall the the corresponding table (from Chuang):

Table 9.1 Summary of the Momentum Matrix Elements in Parabolic Band Model ($|\hat{e}\cdot\mathbf{p}_{cv}|^2 = |\hat{e}\cdot\mathbf{M}|^2$)

Bulk

$$|\hat{x}\cdot\mathbf{p}_{cv}|^2 = |\hat{y}\cdot\mathbf{p}_{cv}|^2 = |\hat{z}\cdot\mathbf{p}_{cv}|^2 = M_b^2 = \frac{m_0}{6}E_p$$

Quantum Well

TE Polarization ($\hat{e}=\hat{x}$ or $\hat{y}$)	**TM Polarization** ($\hat{e}=\hat{z}$)
$\langle|\hat{e}\cdot\mathbf{M}_{c-hh}|^2\rangle = \frac{3}{4}(1+\cos^2\theta)M_b^2$	$\langle|\hat{e}\cdot\mathbf{M}_{c-hh}|^2\rangle = \frac{3}{2}\sin^2\theta M_b^2$
$\langle|\hat{e}\cdot\mathbf{M}_{c-lh}|^2\rangle = (\frac{5}{4}-\frac{3}{4}\cos^2\theta)M_b^2$	$\langle|\hat{e}\cdot\mathbf{M}_{c-lh}|^2\rangle = \frac{1}{2}(1+3\cos^2\theta)M_b^2$

Conservation Rule

$$\langle|\hat{x}\cdot\mathbf{M}_{c-h}|^2\rangle + \langle|\hat{y}\cdot\mathbf{M}_{c-h}|^2\rangle + \langle|\hat{z}\cdot\mathbf{M}_{c-h}|^2\rangle = 3M_b^2, (h = hh \text{ or } lh)$$

$$\langle|\hat{e}\cdot\mathbf{M}_{c-hh}|^2\rangle + \langle|\hat{e}\cdot\mathbf{M}_{c-lh}|^2\rangle = 2M_b^2$$

First set θ=0

TE: LH-X strength is about 1/3 of HH-X

TM: no HH-X abs.

Ref: Chuang

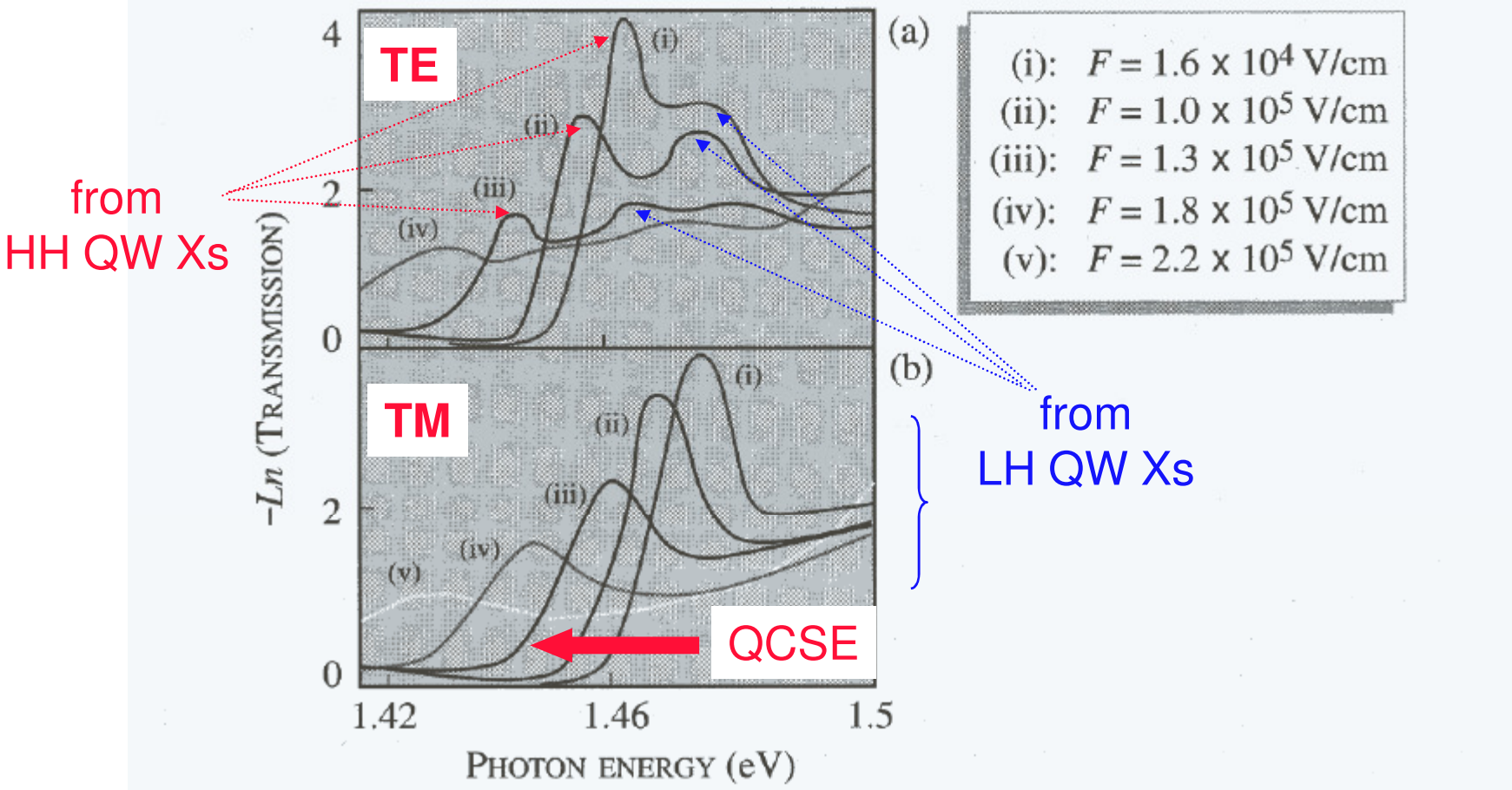

Figure 10.16: Measured polarization dependent transmittances in GaAs/AlGaAs (100 Å) multiquantum well structures when light is coming in the waveguide geometry. (a) Incident polarization parallel to the plane of the layers . (b) Incident polarization perpendicular to the plane of the layers. (After D.A.B. Miller, et al., *IEEE J. Quantum Electronics*, QE-22, 1816 (1986).)

Playing with Strain For Polarization Independence

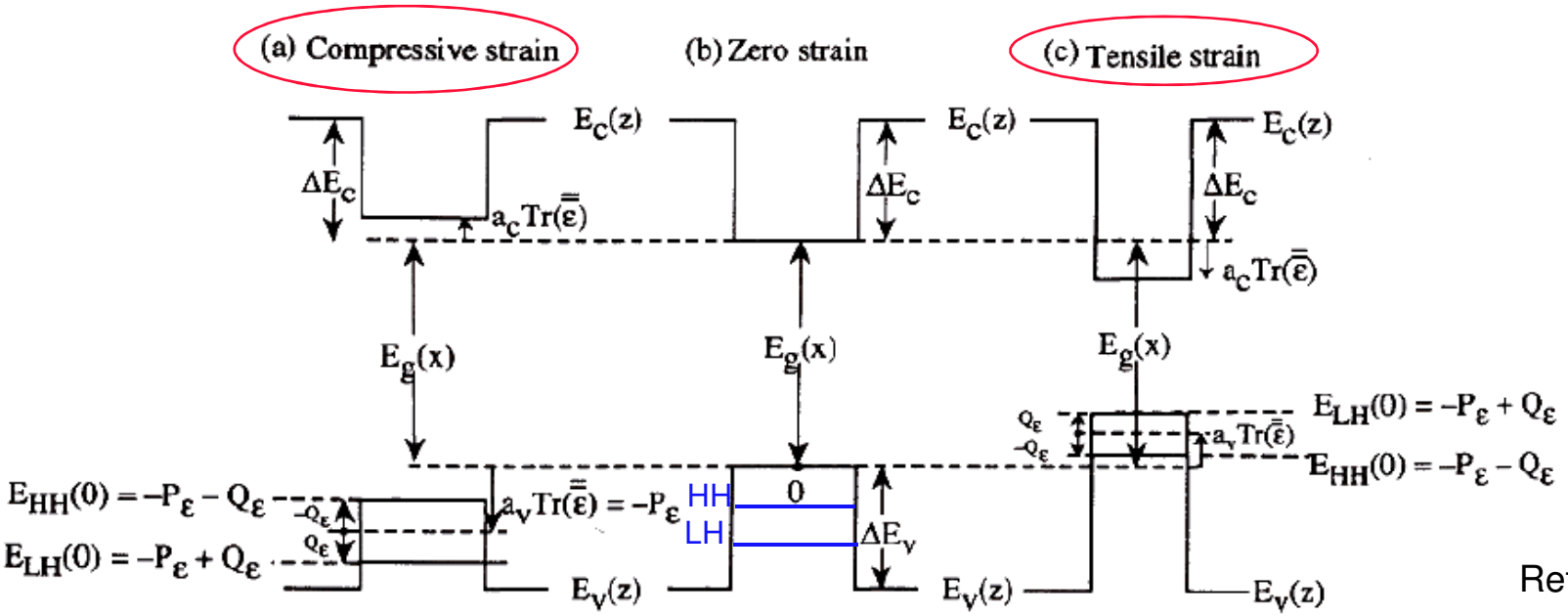

Ref: Chuang

Thus, in principle a properly chosen in-plane tensile strain can cause a merger of the HH and LH states at the zone center in a QW.
Next example demonstrates this case…

An example for strain-polarization

EXAMPLE 10.6 A small tensile strain is used to cause the HH and LH excitonic states to merge in a 100 Å $GaAs/Al_{0.3}Ga_{0.7}As$ well. The quantum well is grown along the (001) direction. Calculate the absorption coefficient for light polarized along the z-direction and along the x (or y) direction. The exciton linewidth is $\sigma = 1.0$ meV.

When the HH and LH states are coincident, the total coupling of the z-polarized light gives, for the momentum matrix element, (see Chapter 9)

$$\frac{2}{3} P_{cv}^2$$

and for the x-polarized light,

$$\frac{1}{2} P_{cv}^2 + \frac{1}{6} P_{cv}^2 = \frac{2}{3} P_{cv}^2$$

In Example 10.2, we calculated the excitonic transition strength using $a_p = \frac{1}{2}$ for x-polarized light, coupling only to the HH state. The absorption strength thus increases to 3.9 $\times 10^4$ cm^{-1} for the peak value.

Ref: Singh

Exciton Quenching: Bulk & QW

1) Quenching of X by free carriers

- A high density of free e's (or h's) is injected into medium containing Xs
- The free carriers screen the Coulombic attraction between e-h, weakening the X binding energy and reducing the X oscillator strength

In bulk (3D), assuming thermodynamic equilibrium yields the following screened e-h attractive potential

$$V_C(r) = -\frac{e^2}{4\pi\varepsilon r}$$

Contains the static screening of the ionic lattice and the valence e's

Screen by free carriers

$$V_{scr}(r) = V_C(r)\, e^{-r/L_D}$$

$$L_D = \sqrt{\frac{\varepsilon k_B T}{n e^2}}$$

Debye screening length

free carrier density

Similarly in QWs, the effect of free carrier screening is to weaken the X binding energy and hence inrease the X radius:

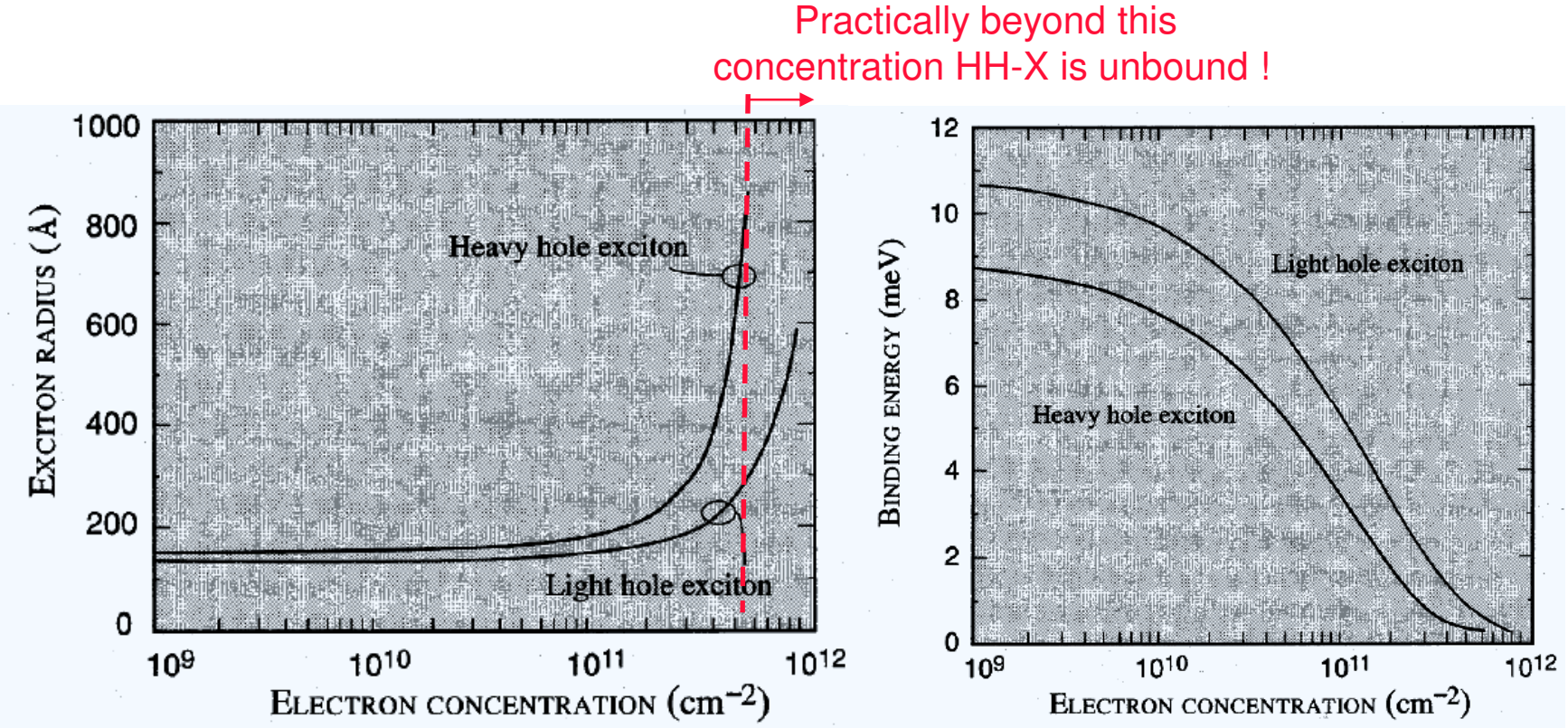

Figure 10.19: (a) Calculated exciton radii a_{ex} in a 100 Å $GaAs/Al_{0.3}Ga_{0.7}As$ quantum well verses electron concentration n_e at $T = 300$ K. (b) Exciton binding energy as a function of carrier concentration.

Ref: Singh

2) Quenching of X by creation of a high density of X

- This is achieved by a high optical illumination
- It gives rise to a gradual saturation of the absorption → NL optics
- This saturation is mainly due to phase space filling and scattering between overlapping Xs among themselves at high densities

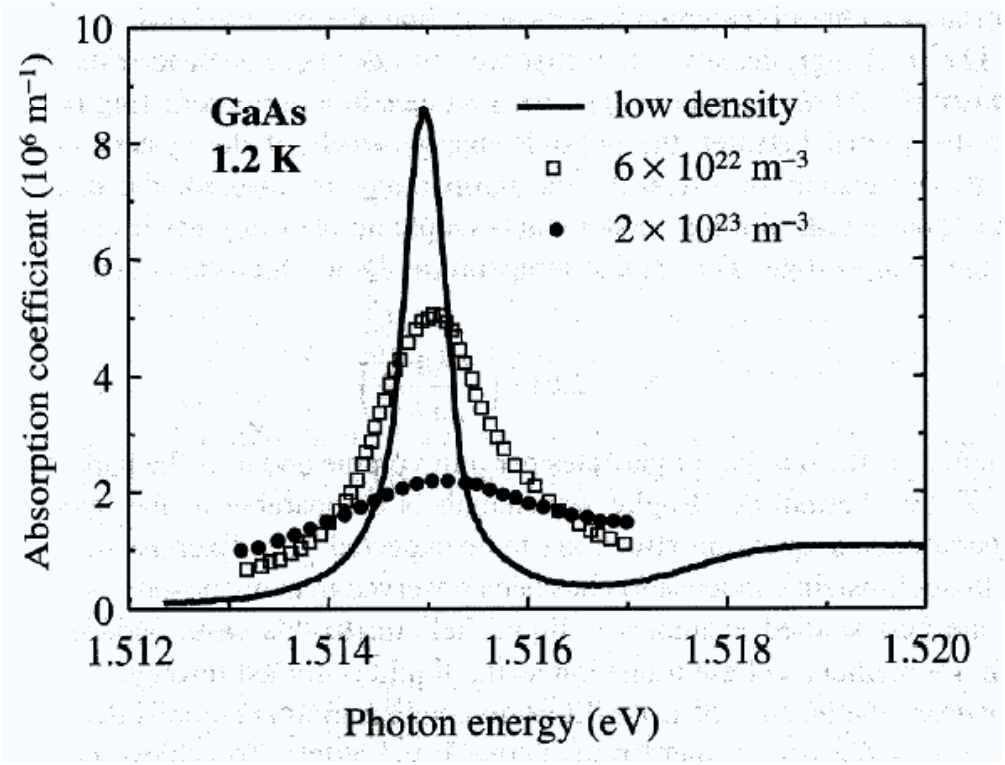

Fig. 4.7 Absorption coefficient of GaAs in the spectral region close to the band edge at 1.2 K at three different excitation powers. The carrier densities generated for the two higher power levels are indicated.

Ref: Fox

What else can happen at high X densities?

➢Another effect that can be observed at high X densities (depending on the material) is the formation of biexcitons (XXs). They have been observed in CdS, ZnSe, ZnO, and especially CuCl

R_x=200 meV
R_{xx}=20 meV

➢In Si and Ge at high densities, yet another effect occurs. At low densities the Xs may be considered to be in gaseous phase. As the density increases, the Xs condense to form a liquid. The liquid phase manifests itself in the formation of electron-hole droplets, which are observed in from the radiation from the recombination of Xs at high densities, The droplet appears as a feature at lower energy than the free X.

Excitons in TMDs

A & B Excitons:

split by spin-orbit interaction

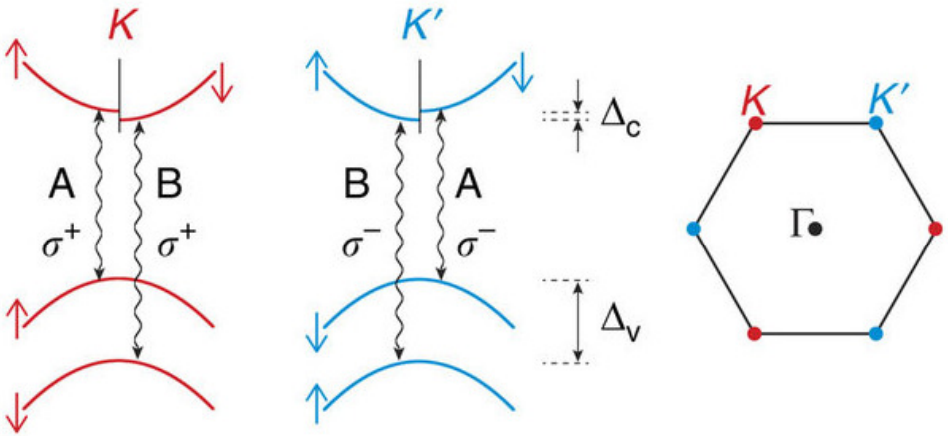

Source: Stier et al. Nature Comm. 2016

WS2 Differential Transmission:

Layer & Temp. dependence

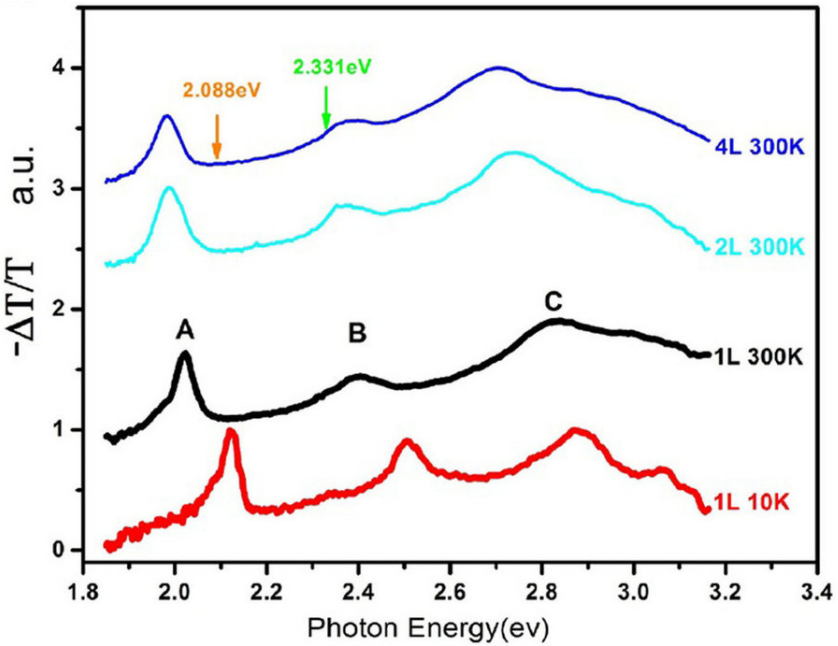

Claimed X binding energy: 710 meV

C exciton couples Γ valleys

Source: Zhu et al. Sci. Rep. 2015

Excitonic Screening in TMDs

PRL **113,** 076802 (2014) PHYSICAL REVIEW LETTERS week ending 15 AUGUST 2014

Exciton Binding Energy and Nonhydrogenic Rydberg Series in Monolayer WS_2

Alexey Chernikov,[1,*] Timothy C. Berkelbach,[2] Heather M. Hill,[1] Albert Rigosi,[1] Yilei Li,[1] Ozgur Burak Aslan,[1] David R. Reichman,[2] Mark S. Hybertsen,[3] and Tony F. Heinz[1,†]

[1]*Departments of Physics and Electrical Engineering, Columbia University, 538 West 120th Street, New York, New York 10027, USA*

[2]*Department of Chemistry, Columbia University, 3000 Broadway, New York, New York 10027, USA*

[3]*Center for Functional Nanomaterials, Brookhaven National Laboratory, Upton, New York 11973-5000, USA*

(Received 12 March 2014; published 13 August 2014)

We have experimentally determined the energies of the ground and first four excited excitonic states of the fundamental optical transition in monolayer WS_2, a model system for the growing class of atomically thin two-dimensional semiconductor crystals. From the spectra, we establish a large exciton binding energy of 0.32 eV and a pronounced deviation from the usual hydrogenic Rydberg series of energy levels of the excitonic states. We explain both of these results using a microscopic theory in which the nonlocal nature of the effective dielectric screening modifies the functional form of the Coulomb interaction. These strong but unconventional electron-hole interactions are expected to be ubiquitous in atomically thin materials.

Source: Chernikov et al. PRL 2014

Excitonic Screening in TMDs

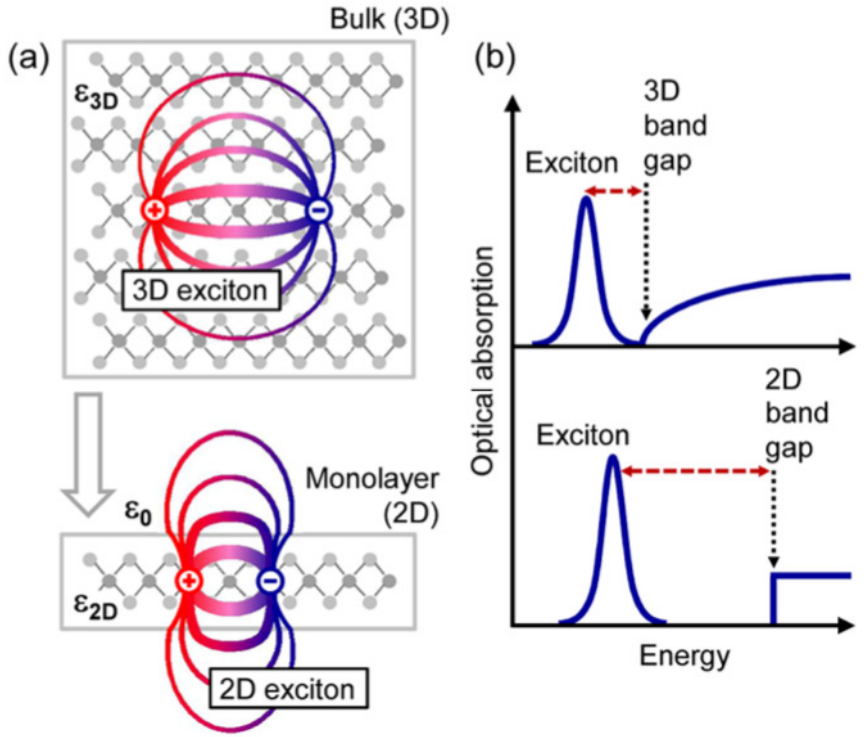

FIG. 1 (color online). (a) Real-space representation of electrons and holes bound into excitons for the three-dimensional bulk and a quasi-two-dimensional monolayer. The changes in the dielectric environment are indicated schematically by different dielectric constants ε_{3D} and ε_{2D} and by the vacuum permittivity ε_0. (b) Impact of the dimensionality on the electronic and excitonic properties, schematically represented by optical absorption. The transition from 3D to 2D is expected to lead to an increase of both the band gap and the exciton binding energy (indicated by the dashed red line). The excited excitonic states and Coulomb correction for the continuum absorption have been omitted for clarity.

Source: Chernikov et al. PRL 2014

Excitonic Screening in TMDs

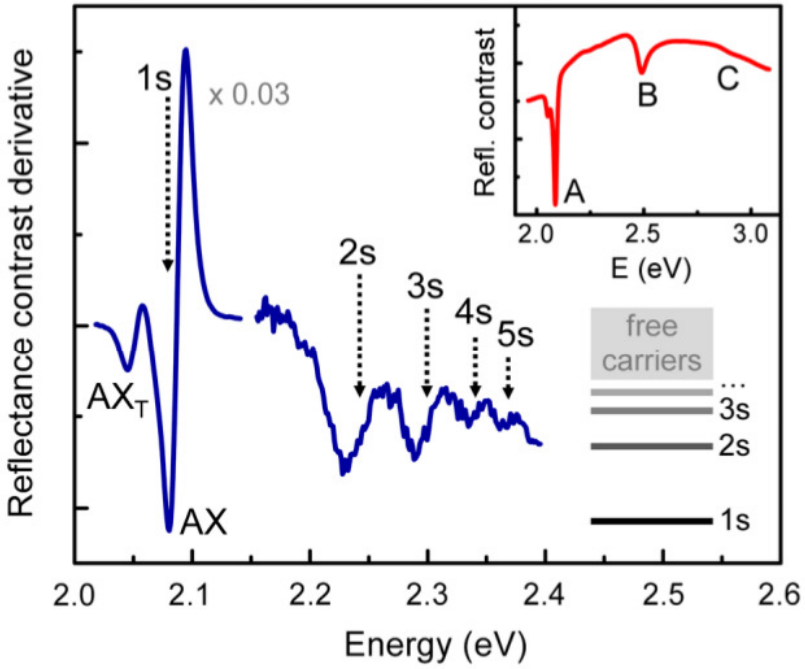

FIG. 2 (color online). The derivative of the reflectance contrast spectrum $(d/dE)(\Delta R/R)$ of the WS_2 monolayer. The exciton ground state and the higher excited states are labeled by their respective quantum numbers (schematically shown at the bottom right). The spectral region around the $1s$ transition (AX) and the trion peak (AX_T) of the A exciton is scaled by a factor of 0.03 for clarity. The inset shows the as-measured reflectance contrast $\Delta R/R$ for comparison, allowing for the identification of the A, B, and C transitions.

Source: Chernikov et al. PRL 2014

Excitonic Screening in TMDs

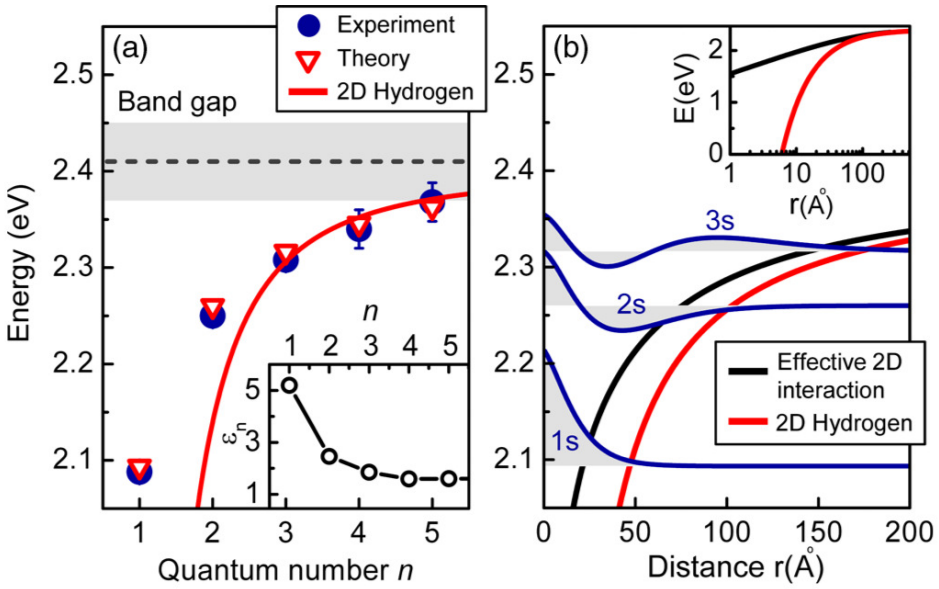

FIG. 3 (color online). (a) Experimentally and theoretically obtained transition energies for the exciton states as a function of the quantum number n. The fit of the $n = 3, 4, 5$ data to the 2D hydrogen model for Wannier excitons is shown for comparison. Gray bands represent uncertainty in the quasiparticle band gap from the fitting procedure. Corresponding effective dielectric constants are shown in the inset. (b) Screened 2D interaction Eq. (2) used in the model Hamiltonian (black lines) compared to the 2D hydrogen interaction $1/r$ (red lines); a semilogarithmic plot is given in the inset. Also shown are the corresponding energy levels and radial wave functions up to $n = 3$. (c) Schematic representation of electron-hole pairs forming $1s$ and $2s$ excitonic states in a nonuniform dielectric environment.

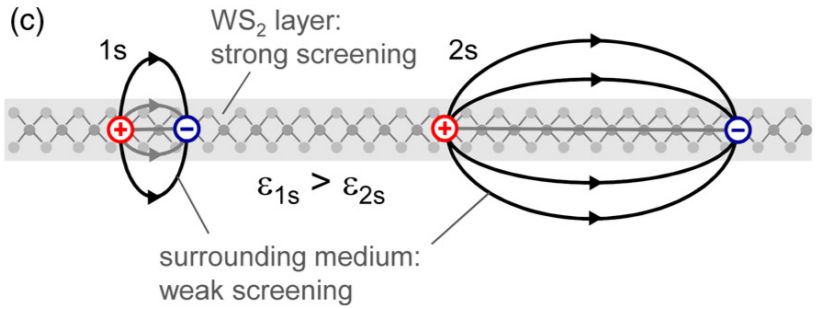

e-h interaction potential

$$V_{e-h}(r) = -\frac{\pi e^2}{2r_0}\left[H_0\left(\frac{r}{r_0}\right) - Y_0\left(\frac{r}{r_0}\right)\right]$$

Sturve & Bessel Fns

1s, 2s outliers; *n*>2 obey 2D H model

Interpolating bet. 1/r (3D) and ln(r) (2D)

Source: Chernikov et al. PRL 2014